



Fractal Dimension of Silhouette Magnetic Resonance Brain Images as a Measure of Age-Associated Changes in Cerebral Hemispheres

Serebral Hemisferdeki Yaşa Bağlı Değişikliklerin Bir Ölçüsü Olarak Silüet Manyetik Rezonans Beyin Görüntülerinin Fraktal Boyutu

Nataliia MARYENKO

 0000-0002-7980-7039

Oleksandr STEPANENKO

 0000-0002-5686-0857

Department of Histology, Cytology
and Embryology, Kharkiv National
Medical University, Kharkiv, Ukraine

ABSTRACT

Aim: The aim of the present study was to characterize age-associated changes in the spatial configuration of cerebral hemispheres (including changes in spatial complexity and space-filling capacity) using fractal analysis of silhouette magnetic resonance brain images.

Material and Methods: Magnetic resonance brain images of 100 (44 male, 56 female) participants aged between 18-86 years were studied. Five magnetic resonance images were selected from the magnetic resonance imaging dataset of each brain, including four tomographic sections in the coronal plane and one in the axial plane. Fractal dimension values of the cerebral hemispheres silhouettes were measured using the two-dimensional box-counting algorithm. Morphometric parameters based on Euclidean geometry (perimeter, area, and their derivative values) were determined as well.

Results: The average fractal dimension value of the five studied tomographic sections was 1.878 ± 0.0009 , the average value of four coronal sections was 1.868 ± 0.0010 . It was shown that fractal dimension values of cerebral silhouettes for all studied tomographic sections and four coronal sections significantly decrease with age ($r = -0.512$, $p < 0.001$ and $r = -0.491$, $p < 0.001$, respectively). The difference in the character of age-related changes in males and females was not statistically significant. Based on the age and the fractal dimension values of the studied sample, the confidence intervals of the fractal dimension values of cerebral hemispheres silhouettes were determined, which can be used as norm criteria in clinical neuroimaging.

Conclusion: The fractal analysis and obtained data can be used in neuroimaging for assessing the degree of age-related cerebral atrophy and for differentiating between normal aging and neurodegenerative diseases.

Keywords: Fractal; cerebrum; aging; atrophy; neuroimaging.

ÖZ

Amaç: Bu çalışmanın amacı, manyetik rezonans beyin görüntülerinden elde edilen silüet görüntülerin fraktal analizini kullanarak serebral hemisferlerin uzaysal konfigürasyonundaki yaşa bağlı değişiklikleri (uzaysal karmaşıklık ve boşluk doldurma kapasitesindeki değişiklikler dahil) tanımlamaktır.

Gereç ve Yöntemler: Yaşları 18-86 yıl arasında olan 100 (44 erkek, 56 kadın) katılımcının manyetik rezonans beyin görüntüleri incelenmiştir. Her bir beyin manyetik rezonans görüntülemeye, koronal düzlemde dört tomografik kesit ve aksiyal düzlemde bir kesit dahil olmak üzere beş manyetik rezonans görüntüsü seçildi. Serebral hemisfer silüetlerinin fraktal boyut değerleri, iki boyutlu kutu sayma algoritması kullanılarak ölçüldü. Öklid geometrisine dayalı morfometrik parametreler (çevre, alan ve bunlardan türetilen değerler) de belirlendi.

Bulgular: Çalışılan beş tomografik kesitin ortalama fraktal boyut değeri $1,878 \pm 0,0009$ ve dört koronal kesitin ortalama değeri ise $1,868 \pm 0,0010$ idi. İncelenen tüm tomografi kesitleri ve dört koronal kesit için serebral silüetlerin fraktal boyut değerlerinin yaş ile birlikte anlamlı olarak azaldığı gösterildi (sırasıyla $r = -0,512$, $p < 0,001$ ve $r = -0,491$, $p < 0,001$). Erkeklerde ve kadınlarda yaşa bağlı değişikliklerin karakterindeki fark istatistiksel olarak anlamlı değildi. Çalışılan örneğin yaş ve fraktal boyut değerleri esas alınarak, serebral hemisfer silüetlerinin fraktal boyut değerleri için klinik nörogörüntüleme norm kriteri olarak kullanılabilir güven aralıkları belirlendi.

Sonuç: Fraktal analiz ve elde edilen veriler, yaşa bağlı serebral atrofi derecesini değerlendirmek ve normal yaşlanma ile nörodejeneratif hastalıklar arasında ayırım yapmak için nörogörüntüleme kullanılabilir.

Anahtar kelimeler: Fraktal; beyin; yaşlanma; atrofi; nöro-görüntüleme.

Corresponding Author
Sorumlu Yazar

Nataliia MARYENKO
maryenko.n@gmail.com

Received / Geliş Tarihi : 27.09.2022

Accepted / Kabul Tarihi : 16.01.2023

Available Online /

Çevrimiçi Yayın Tarihi : 17.02.2023

Presented orally at the Ukrainian Scientific-Practical Conference: Morphogenesis and Regeneration of Human and Animals Organs in the Norm, with Pathology and Under the Correction (April 14, 2022; Poltava, Ukraine).

INTRODUCTION

Among the various structures and formations in the human body, the cerebrum has one of the most sophisticated shapes reflecting the complexity of its morphofunctional organization (1,2). During adulthood, morphological changes occur in different brain structures, reflecting its development and aging (3-5). Brain aging is accompanied by mostly atrophic changes, affecting the shape and dimensions of brain structures (3-5). Quantitative characterization of age-related changes in the brain shape is an important area of clinical neuroscience and neuro-morphology research (3-5). This is necessary both for determining the degree of atrophy and for differentiating changes in normal aging and in neurodegenerative diseases (3-7).

Numerous studies aimed to characterize and quantify brain structures using traditional morphometric methods, including volumetric studies, measurements of gray and white matter volumes (8-12), assessment of the cortical thickness (11-13), sulcal depth (12,13), and gyrification index, the ratio of the total brain surface to the superficially exposed brain surface (11,13-15). But the spatial configuration of the cerebral hemispheres is too irregular and difficult to be comprehensively assessed using morphometric methods based on Euclidean geometry (1,2,16).

In recent decades, the cerebral cortex and its configuration have been considered by scientists as a natural fractal (14-16). Therefore, for a comprehensive study of irregular structures, such as the cerebrum, various methods and modifications of fractal analysis were used (2,12-31). Fractal analysis is a method of mathematical analysis that quantitatively characterizes the structural complexity of geometric figures and their space-filling degree (1,2). The main parameter determined by fractal analysis is the fractal dimension (FD) which can be described as a measure of the space-filling capacity of the studied irregular geometric figures (1). In previous studies, various researchers used fractal analysis to study the cerebral cortical ribbon (14-20), the pial surface of the cerebral cortex (19-26), the cerebral white matter (20,27-31), including its outer surface, the linear boundary between cortical ribbon and white matter (20,30,31). However, despite the diversity of studies involving fractal analysis of brain structures, the whole silhouettes of cerebral hemispheres haven't been studied before.

In this study, we aimed to characterize age-associated changes in the spatial configuration of cerebral hemispheres (including changes in spatial complexity and space-filling capacity) using fractal analysis of silhouette magnetic resonance (MR) brain images.

MATERIAL AND METHODS

The present study was approved by the Commission on Ethics and Bioethics of Kharkiv National Medical University (No.10 of Nov 7, 2018).

MR brain images obtained from 100 (44 male, 56 female) participants with an 18-86 years age range were studied. Thirty-one (14 male, 17 female) of which were between 18-30 years, 29 (14 male, 15 female) were between 31-45 years, 24 (8 male, 16 female) were between 46-60 years, and 16 (8 male, 8 female) were between 61-86 years. The mean age was 41.72 ± 1.78 years. The mean age for male

participants was 41.43 ± 1.68 (range, 18-86) years and 41.95 ± 1.51 (range, 18-72) years for female participants. Patients of the studied sample underwent diagnostic magnetic resonance imaging (MRI) brain scanning and showed no apparent brain pathology upon examination. Their MRI data were considered as relatively normal. The exclusion criterion was the presence of pathological structural changes in the brain and surrounding structures.

Magnetic Resonance Imaging (MRI) Protocol

MRI was performed on a 1.5 T MRI machine (Siemens Magnetom Symphony). T2 and FLAIR sequences were chosen. MRI parameters were T2 sequence: TE (echo time) 130 ms, TR (repetition time) 4440 ms, and FLAIR sequence: TE (echo time) 114 ms, TR (repetition time) 9000 ms, TI (inversion time) 2500 ms. The slice (section) thickness for both MRI sequences was 5 mm. The resolution of digital MR brain images was 72 dpi.

Selection of Tomographic Sections

Five MR images were selected from the MRI dataset of each brain, including four tomographic sections in the coronal (frontal) plane and one in the axial (horizontal) plane. A total of 500 MR brain images were selected. Selection criteria were: location in different parts of the cerebral hemispheres, easy identification by anatomical landmarks, the inclusion of brain areas where pathological lesions are most often found in some neurodegenerative diseases, including Alzheimer's disease (15). The 1st coronal section (Coronal 1) was located at the level of the anterior points of the temporal lobes, the 2nd (Coronal 2) at the level of the mamillary bodies (corpus mamillare), the 3rd (Coronal 3) at the level of the quadrigeminal plate (lamina quadrigemina), and the 4th (Coronal 4) at the level of corpus callosum posterior pole (splenium corporis callosi). The axial section was selected as an uppermost horizontal tomographic section intercepting the thalamus (due to the section thickness of 5 mm this section was located at the upper part of the thalamus).

Image Pre-processing

Blank frame images were created using the Adobe Photoshop CS5 graphics editor. The size of the frame image was 512×400 pixels for coronal sections, and 512×800 pixels for axial. The absolute scale of the digital images was the following: 3 pixels (voxels) = 1 mm. The fragments of digital MR images were inserted into the blank frame images; the tomographic sections of cerebral hemispheres were completely placed in the frames and did not go beyond them (Figure 1, A). The structures surrounding the sections of cerebral hemispheres were initially removed from the images (Figure 1, B), and the pixels in these areas were colored white (pixel intensity value of 255) for the T2 sequence or black (pixel intensity value of 0) for the FLAIR sequence. Preliminary ("rough") segmentation was provided by image thresholding. The pixel intensity threshold value was 128 for the T2 sequence, and 65 for the FLAIR sequence. As a result of thresholding, grayscale MR images were converted into binary. Precise segmentation was performed to improve the anatomical accuracy of the obtained silhouette brain images (Figure 1, C). This was done using a manual correction by Adobe Photoshop CS5 tools. The preprocessing procedure was done for 500 selected images.

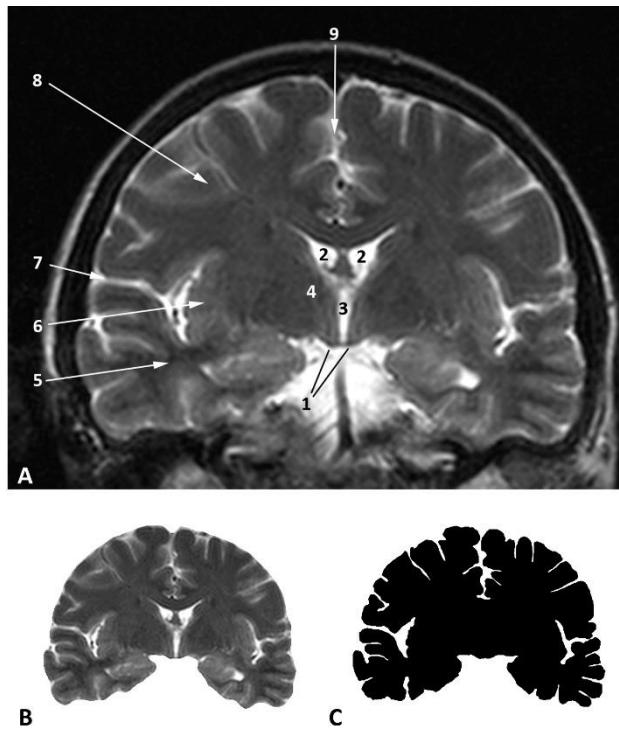


Figure 1. Pre-processing of magnetic resonance brain image (37 years old female). **A)** magnetic resonance image of cerebral hemispheres (Coronal 2, level of mamillary bodies), 1: mamillary bodies, 2: lateral ventricles, 3: 3rd ventricle, 4: thalamus, 5: temporal lobe, 6: insula, 7: lateral sulcus, 8: parietal lobe, 9: longitudinal cerebral fissure; **B)** non-segmented tomographic section after background removal; **C)** segmented silhouette image

Fractal Analysis

Fractal analysis was carried out using the 2D box-counting method tool of the Image J software (32). The FD values of the silhouette images of five different (Coronal 1 to 4,

and Axial) localizations were determined for each participant (Figure 2). The average FD value of all five sections and the average FD value of four coronal sections were also calculated.

Euclidean-Based Image Morphometry

Morphometric parameters based on Euclidean geometry were determined on two types of images. 1st type of images-non-segmented tomographic sections (Figure 1, B), the perimeter of which corresponds to the contour of the superficially exposed surface of cerebral hemispheres, and the area corresponds to the brain tissue as a whole, including the contents of the sulci. The following parameters were determined in these images: P_0 (perimeter), A_0 (area), P_0/A_0 (perimeter-to-area ratio), and SF_0 (shape factor). 2nd type of images-segmented silhouette images (Figure 1, C), the perimeter of which corresponds to the contour of the whole pial surface of the cerebral hemispheres (including the pial surface contour inside the sulci), and the area corresponds to the brain tissue as a whole (but not including the contents of the sulci). The following parameters were determined in these images: P_s (perimeter), A_s (area), P_s/A_s (perimeter-to-area ratio), and SF_s (shape factor). To determine the shape factor for both types of images we used the formula: " $SF=(4\pi \times A)/P^2$ " (33). The ratios of the perimeter and the area of segmented silhouette images to the corresponding parameters of non-segmented images were also calculated (P_s/P_0 and A_s/A_0 , respectively).

Statistical Analysis

Statistical data processing was done using Excel 2016 software. The mean, standard error of the mean, standard deviation, coefficient of variation (CV, relative standard deviation), median, 25th and 75th percentiles values, and minimum-maximum values were calculated. The normality of distribution was verified using the Shapiro-Wilk test. The statistical significance of the difference between FD values measured in different tomographic sections was

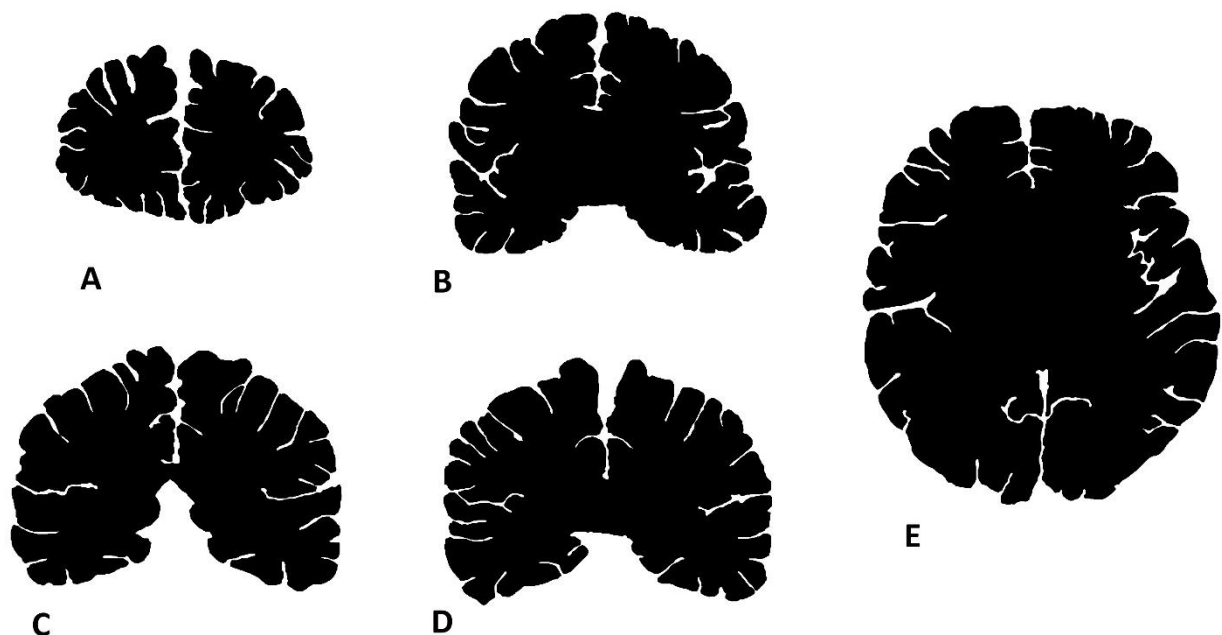


Figure 2. Silhouette images of cerebral hemispheres revealed after preprocessing of magnetic resonance images of different localization (36 years old female). **A)** Coronal 1, level of temporal lobes anterior pole; **B)** Coronal 2, level of mamillary bodies; **C)** Coronal 3, level of the quadrigeminal plate; **D)** Coronal 4, level of corpus callosum posterior pole (splenium corporis callosi); **E)** Axial, thalamus level

assessed using the Kruskal-Wallis H test and post-hoc Dunn's test with Bonferroni adjustment for multiple comparisons. The statistical significance of the difference between FD values and the age of sex groups were verified using the Mann-Whitney U test. The statistical significance of the difference between the linear regression equations was assessed using Fisher's F test. To characterize the correlation, Pearson's correlation coefficient was calculated, the significance of which was assessed using the Student's t-test. The significance level for all results was accepted as $p < 0.05$.

RESULTS

Fractal Dimension Values

The statistical descriptive parameters of FD values obtained in the present study were shown in Table 1. The FD values of the cerebral hemispheres had low values of the variation coefficient (0.39% to 1.01%), which indicates low variability of the cerebral FD.

The distributions of FD values were verified for normality and it was found that the distributions of FD values of the sections Coronal 1 and Coronal 2 did not differ significantly from the normal distribution ($p=0.310$, and $p=0.281$, respectively). The distribution of FD values of the sections Coronal 3 and Axial were significantly different from the normal distribution ($p=0.018$, and $p=0.036$, respectively). The difference between the distribution of FD values of the Coronal 4 section and the normal distribution was questionable ($p=0.059$). The distributions of the average FD values of the five sections and the average FD values of the four coronal

sections were significantly different from the normal distribution ($p=0.001$ for both values).

Since distributions of FD values of some tomographic sections were significantly different from the normal distribution, we chose the non-parametric Mann-Whitney U test to assess the statistical significance of the difference between FD values measured in male and female sex groups (Table 1). It indicated that mean ranks of FD values determined in female and male sex groups were not significantly different in all studied tomographic sections, Coronal 1 $p=0.168$, Coronal 2 $p=0.811$, Coronal 3 $p=0.177$, Coronal 4 $p=0.352$, Axial $p=0.361$, average FD values of the five sections $p=0.992$, average FD values of the four coronal sections $p=0.811$. We also compared the age of male and female sex groups using the Mann-Whitney U test, which indicated that mean ranks of age in male and female sex groups of the studied sample were not significantly different ($p=0.811$). Taking into account the absence of the difference between age and FD values of males and females, we used a non-divided sample for a few following analyses.

In the next stage of the study, we compared the FD values of five tomographic sections. The highest FD values were determined in the Axial section, and the lowest FD values were determined in the Coronal 1 section. There was a significant difference between the FD values of five sections ($p < 0.001$). The post-hoc comparison indicated that the mean ranks of the FD values of the following section pairs were significantly different, Coronal 1 vs Coronal 2, Coronal 1 vs Coronal 3, Coronal 1 vs Coronal 4, Coronal 1 vs Axial, Coronal 2 vs Axial, Coronal 3 vs Axial,

Table 1. Statistical parameters of fractal dimension values of cerebral hemispheres silhouette images

Section	Sex Group	Mean	SE	SD	CV (%)	Median	Q1-Q3	Min-Max
Coronal 1	Both	1.851	0.0016	0.016	0.84	1.852	1.841-1.862	1.809-1.885
	Male	1.848	0.0028	0.019	1.01	1.850	1.834-1.862	1.809-1.885
	Female	1.853	0.0017	0.012	0.67	1.854	1.846-1.862	1.825-1.880
Coronal 2	Both	1.874	0.0013	0.013	0.68	1.874	1.866-1.882	1.840-1.900
	Male	1.874	0.0018	0.012	0.65	1.874	1.868-1.884	1.840-1.896
	Female	1.873	0.0018	0.013	0.71	1.875	1.865-1.881	1.843-1.900
Coronal 3	Both	1.872	0.0014	0.014	0.75	1.874	1.864-1.880	1.834-1.905
	Male	1.873	0.0025	0.016	0.88	1.877	1.863-1.885	1.838-1.905
	Female	1.871	0.0016	0.012	0.64	1.873	1.865-1.878	1.834-1.898
Coronal 4	Both	1.876	0.0013	0.013	0.69	1.877	1.869-1.884	1.842-1.904
	Male	1.877	0.0022	0.015	0.79	1.880	1.868-1.885	1.842-1.904
	Female	1.875	0.0015	0.011	0.60	1.875	1.869-1.883	1.846-1.897
Axial	Both	1.918	0.0009	0.009	0.47	1.919	1.913-1.924	1.889-1.936
	Male	1.917	0.0013	0.009	0.44	1.919	1.913-1.922	1.893-1.933
	Female	1.919	0.0012	0.009	0.48	1.920	1.913-1.926	1.889-1.936
Average (All Sections)	Both	1.878	0.0009	0.009	0.48	1.880	1.873-1.884	1.852-1.894
	Male	1.878	0.0016	0.011	0.58	1.879	1.874-1.885	1.852-1.893
	Female	1.878	0.0010	0.007	0.39	1.880	1.873-1.883	1.859-1.894
Average (Coronal 1-4)	Both	1.868	0.0010	0.010	0.55	1.870	1.862-1.875	1.840-1.888
	Male	1.868	0.0019	0.012	0.66	1.870	1.863-1.877	1.840-1.887
	Female	1.868	0.0011	0.008	0.45	1.870	1.862-1.874	1.845-1.888

SE: standard error of the mean, SD: standard deviation, CV: coefficient of variation (relative standard deviation), Q1-Q3: 25th-75th percentile, min: minimum, max: maximum

and Coronal 4 vs Axial ($p < 0.001$ for all). It also indicated that the mean ranks of the FD values of the following section pairs were not significantly different, Coronal 2 vs Coronal 3 ($p = 0.570$), Coronal 2 vs Coronal 4 ($p = 0.378$), Coronal 3 vs Coronal 4 ($p = 0.147$).

Correlation Analysis

Significant positive correlations were found between the FD values of Coronal 1 and Coronal 2, Coronal 1 and Coronal 3, Coronal 1 and Coronal 4, Coronal 2 and Coronal 3, Coronal 2 and Coronal 4, Coronal 3 and Coronal 4, Coronal 3 and Axial, and Coronal 4 and Axial section pairs (Table 2). The highest correlation coefficient values were found between the FD values of adjacent coronal tomographic sections, Coronal 3 and Coronal 4, and Coronal 2 and Coronal 3. No statistically significant correlations were found between the FD values of the Coronal 1 and Axial, and Coronal 2 and Axial section pairs.

Correlations between the FD values and the morphometric parameters of non-segmented tomographic sections were analyzed (Table 3). Significant positive correlations were found between the FD values and values of area (A_0) and shape factor (SF_0) in coronal sections. The correlations between FD values and perimeter values (P_0) were significant only in the sections Coronal 3 and Coronal 4. Significant negative correlations were found between the FD values and perimeter-to-area ratio (P_0/A_0) in coronal sections.

We also analyzed correlations between the FD values and the morphometric parameters of segmented silhouette images (Table 3). Significant positive correlations were found between the FD values and values of area (A_s) and shape factor (SF_s) in all studied sections. Significant negative correlations were found between the FD values and perimeter-to-area ratio (P_s/A_s) in all sections. The perimeter values (P_s) didn't have a significant correlation with FD values in coronal sections, but there was a

significant negative correlation between these values in the Axial section. Significant positive correlations between the FD values and the two-dimensional gyrification index (ratio of perimeters, P_s/P_0) were found only in the Axial section. Also, significant correlations were found between the FD values and the ratio of the areas (A_s/A_0) in all coronal sections.

To study changes in the spatial configuration of the cerebral hemispheres, we conducted a correlation analysis between the FD values and age. We found negative significant correlations between those parameters. It indicates a tendency for FD values to decrease with age. Figure 3 illustrates FD values distribution throughout adulthood. The strongest correlations between age and FD were found in the sections Coronal 2 ($r = -0.511$, $p < 0.001$) and Coronal 3 ($r = -0.429$, $p < 0.001$). Weak correlations were found in the sections Coronal 1 ($r = -0.232$, $p < 0.05$), Coronal 4 ($r = -0.312$, $p < 0.001$), Axial ($r = -0.313$, $p < 0.001$). Also, we found moderate negative significant correlations between the age and the average FD values of all five tomographic sections ($r = -0.512$, $p < 0.001$) and the average FD values of four coronal sections ($r = -0.491$, $p < 0.001$).

Table 2. Correlation of the cerebral silhouettes fractal dimension values measured in different tomographic sections

Section	Coronal 1	Coronal 2	Coronal 3	Coronal 4
Coronal 2	r	0.249		
	p	0.012		
Coronal 3	r	0.333	0.440	
	p	<0.001	<0.001	
Coronal 4	r	0.367	0.351	0.701
	p	<0.001	<0.001	<0.001
Axial	r	0.104	0.155	0.425
	p	0.303	0.124	<0.001

Table 3. Correlation of the cerebral silhouettes fractal dimension values and values of Euclidean geometry-based morphometric parameters of cerebral hemispheres

Type of Image	Morphometric Parameter	Tomographic Section of Cerebral Hemispheres					
		Coronal 1	Coronal 2	Coronal 3	Coronal 4	Axial	
Non-segmented Tomographic Sections	Perimeter (P_0)	r	0.079	0.129	0.228	0.209	0.166
		p	0.435	0.201	0.023	0.036	0.099
	Area (A_0)	r	0.242	0.230	0.434	0.389	0.094
		p	0.015	0.021	<0.001	<0.001	0.352
	Perimeter-to-area ratio (P_0/A_0)	r	-0.319	-0.275	-0.478	-0.477	0.113
		p	0.001	0.006	<0.001	<0.001	0.263
	Shape Factor (SF_0)	r	0.376	0.133	0.258	0.316	-0.035
		p	<0.001	0.187	0.010	0.001	0.730
Segmented Silhouette Images	Perimeter (P_s)	r	-0.029	0.009	0.072	0.039	-0.285
		p	0.775	0.929	0.477	0.700	0.004
	Area (A_s)	r	0.446	0.463	0.694	0.600	0.388
		p	<0.001	<0.001	<0.001	<0.001	<0.001
	Perimeter-to-area ratio (P_s/A_s)	r	-0.519	-0.410	-0.509	-0.503	-0.610
		p	<0.001	<0.001	<0.001	<0.001	<0.001
	Shape Factor (SF_s)	r	0.339	0.231	0.246	0.276	0.467
		p	<0.001	0.021	0.014	0.005	<0.001
Both Types of Images	Ratio of perimeters (P_s/P_0) (2D gyrification index)	r	-0.082	-0.072	-0.050	-0.088	-0.426
		p	0.417	0.477	0.621	0.384	<0.001
	Ratio of areas (A_s/A_0)	r	0.573	0.628	0.605	0.590	0.156
		p	<0.001	<0.001	<0.001	<0.001	0.121

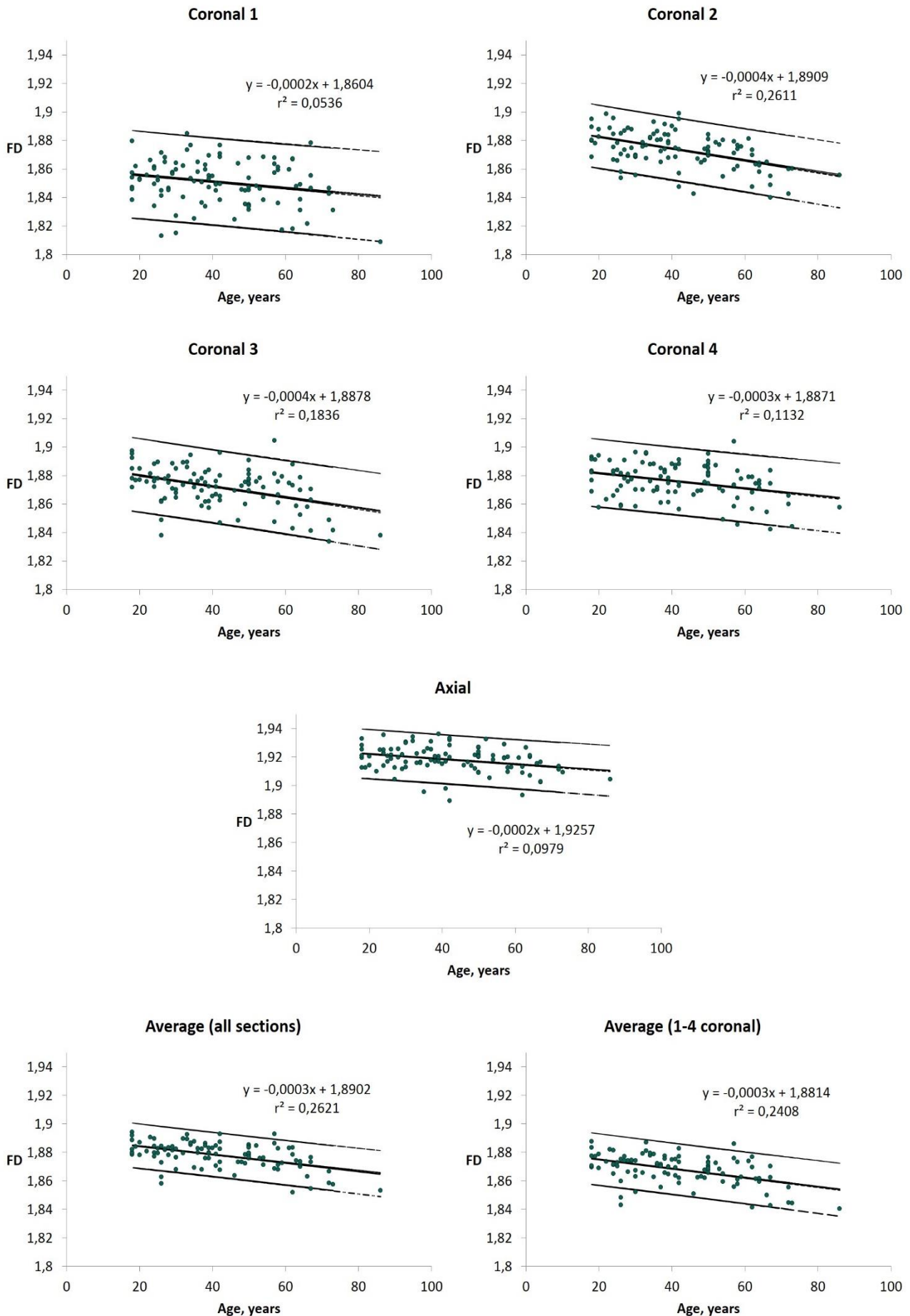


Figure 3. Fractal dimension values of cerebral silhouettes, changes throughout adulthood, confidence intervals, and linear regression equations in different tomographic sections

Figure 4 shows two silhouette images of the cerebral hemispheres of young and old persons (23 and 72 years old, respectively). We can notice the age-associated atrophic changes in the silhouette brain image of the older person, the widening and deepening of the sulci, and the atrophic changes in the gyri shape. The FD values of these images were significantly different, the FD value of the young person was 1.88, and the FD value of the old person was 1.85.

As we have noticed earlier, FD values determined in the male and female groups of the studied sample were not significantly different as well as age. Additionally, we analyzed the relationships of FD values with age in the male and female groups (Figure 5). Negative correlations were found between FD values and age in both sex groups in all studied tomographic sections: $r=-0.292$, $p=0.054$ for males, and $r=-0.174$, $p=0.120$ for females in the Coronal 1 section; $r=-0.573$, $p<0.001$ for males, and $r=-0.465$, $p<0.001$ for females in the Coronal 2 section; $r=-0.431$, $p=0.003$ for males, and $r=-0.432$, $p<0.001$ for females in the Coronal 3 section; $r=-0.317$, $p=0.036$ for males, and $r=-0.307$, $p=0.021$ for females in the Coronal 4 section; $r=-0.502$, $p<0.001$ for males, and $r=-0.174$, $p=0.120$ for females in the Axial section; $r=-0.526$, $p<0.001$ for males, and $r=-0.508$, $p<0.001$ for females for the average FD values of all five tomographic sections; $r=-0.489$, $p<0.001$ for males, and $r=-0.505$, $p<0.001$ for females for the average FD values of four coronal sections. The character of correlations in female and male groups was close to that determined in the undivided sample. The correlation coefficients determined in male and female groups were close to each other almost in all studied sections (except the Axial section, females showed no significant correlations between FD value and age). However, in addition to the strength and character of correlations, it is important to compare the dynamics of age-related changes in FD in the studied groups. We calculated linear regression equations characterizing age dynamics of FD values (FD value was the response variable, and age was the predictor variable) and compared obtained equations in female and male groups (Figure 5). The analysis showed that linear regression equations were not significantly different in males and females in all studied tomographic sections ($p\approx 1$ for all sections).

DISCUSSION

In this study, we have described features of age-associated changes in cerebral hemispheres using fractal analysis of MR silhouette brain images. We have found that the FD values of cerebral silhouettes significantly decrease with age. Our findings are consistent with data from some previous studies, which have shown that FD values of different brain structures had significant negative correlations with age (12,21,29,30).

Some studies regarding age-related changes in fractal measurements involved the assessment of the cortical ribbon or the cortical surface (12,21,22).

The study of Podgórski et al. (12) included the comparative analysis of brain aging using methods of fractal and Euclidean geometry-based morphometries. The brain MR images of healthy volunteers were studied. The following parameters were measured to assess the aging changes: volumes of total gray matter, white matter and

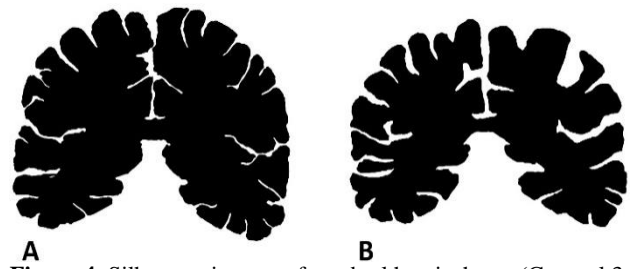


Figure 4. Silhouette images of cerebral hemispheres (Coronal 3, level of quadrigeminal plate) of young and old persons. **A)** 23 years old male with a fractal dimension value of 1.88, **B)** 72 years old male with a fractal dimension value of 1.85

cerebrospinal fluid, cortical thickness, sulcal depth, gyrification index, and FD. The authors described a decrease in gray and white matter volumes and an increase in cerebrospinal fluid volume. Cortical thickness and gyrification index decreased with age, meanwhile, the sulcal depth increased. The authors also investigated cortical maps of the age-related distribution of FD and found that FD was changed during aging.

The study of Madan and Kensinger (21) aimed to examine differences in cortical complexity across the adult lifespan. The authors used a three-dimensional box-counting algorithm for the fractal analysis of the MR brain images. The study revealed that the FD of the cortical ribbon significantly decreased with age ($r=-0.732$) as well as the FD of the cortical surface ($r=-0.719$), mean cortical thickness ($r=-0.603$), and gyrification index ($r=-0.494$). The authors also estimated correlation relationships and found that values of the correlation index between FD of the cortical ribbon and cortical thickness, FD, and gyrification index were $r=0.863$ and $r=0.626$, respectively. In the study of Kalmanti and Maris (22) two-dimensional fractal analysis of the cerebral cortex was provided. Parasagittal tomographic sections were used for the measurements. The studied sample included 93 persons aged from 3 months to 78 years (mainly children and adolescents). The authors demonstrated differences in two-dimensional FD between ages, possibly related to brain development.

The study of Im et al. (25) involved fractal analysis of the three-dimensional cortical surface, using the box-counting method. The authors showed significant correlation relationships of the FD of the cortical surface with cortical thickness, sulcal depth, and folding area. Also, an interesting finding of this study was the correlation of FD with intelligence quotient and the number of education years; the results showed that the FD of the cortical surface had a significant relationship with intelligence and education.

Cortex and cortical ribbon were studied in the studies regarding the atrophic changes in neurodegenerative diseases. In the studies of King et al. (15,19) cerebral cortical ribbons in Alzheimer's disease were studied by two-dimensional and three-dimensional box-counting algorithms of fractal analysis. The authors quantified atrophic changes in cerebral hemispheres and described the significant difference between FDs of the cortical ribbon of healthy persons and patients with Alzheimer's disease. Fractal analysis of the cortex and cortical ribbon

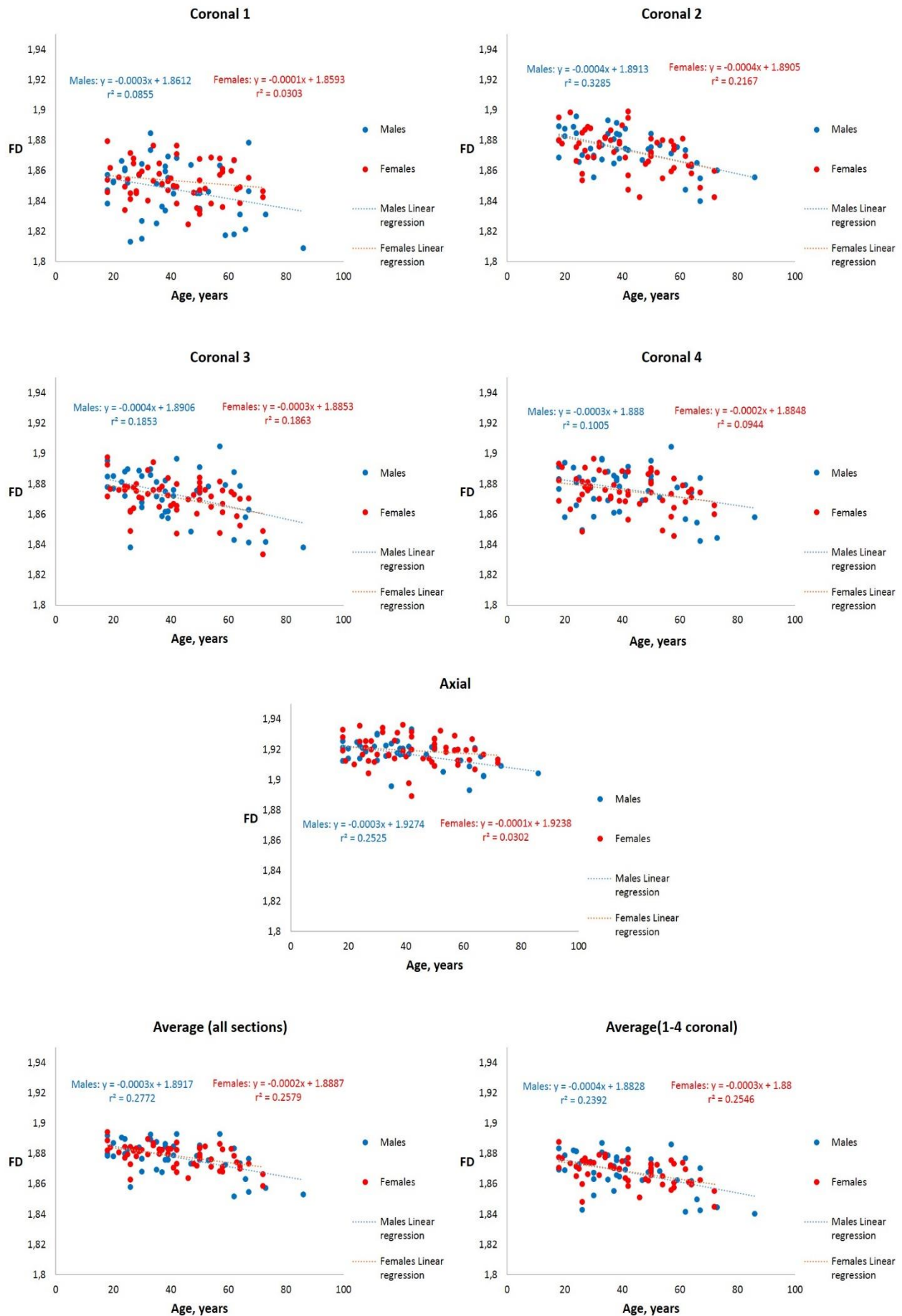


Figure 5. Fractal dimension values of cerebral silhouettes in female and male sex groups, changes throughout adulthood, and linear regression equations in different tomographic sections

also revealed significant changes in patients with multiple sclerosis (17,18), schizophrenia and obsessive-compulsive disorder (23), and auditory verbal hallucinations (24).

Other studies on age-dependent changes of the FD were focused on the brain white matter (29,30). In the study of Zhang et al. (29), a three-dimensional modification of the box-counting method was applied for the fractal analysis of MR brain images. The authors measured the FD of white matter volume (whole white matter), surface (white matter/gray matter boundary), and skeletonized white matter images. There were significant differences between FD values of white matter volume, surface, and skeleton between young and old persons.

In the study of Farahibozorg et al. (30) cerebral white matter was studied. The authors used a three-dimensional box-counting method to provide fractal analysis of brain MR images. In each brain, three FD values were measured, general (volume, whole white matter), skeleton, and boundaries (surface, white matter/gray matter boundary). FDs of white matter volume and skeleton showed inverse U-shape patterns with aging ($r^2=0.116$ for general FD, $r^2=0.202$ for skeleton FD), and FD of white matter surface was less affected by age ($r^2=0.040$). The authors found positive correlations between FD and white matter volume, $r=0.480$ for general FD, $r=0.558$ for skeleton FD, and $r=0.385$ for boundary FD.

Fractal analysis of cerebral white matter was also provided in some diseases and pathological conditions, significant changes were found in patients with multiple sclerosis (27) and traumatic brain injury (28).

Some studies involved the assessment of both white and gray matter. The study of Goñi et al. (20) aimed to quantify the reliability of fractal measures within the human brain. Authors in their study used MR brain images and measured the FDs of the pial cortical surface, the cortical ribbon volume, the white matter volume, and the gray matter/white matter boundary. The three-dimensional box-counting method was used for the fractal analysis. The authors estimated three different FDs (the Kolmogorov capacity dimension, the information dimension, and the correlation dimension) and concluded that the highest reproducibility was achieved with the correlation dimension.

The three-dimensional box-counting algorithm is the most commonly used fractal analysis method in recent studies. It has its undeniable advantages, as it determines a single FD value of the whole cortical ribbon or whole cerebral white matter or whole surface of cerebral hemispheres (19-21,25,29-31). Most three-dimensional fractal analysis algorithms require the construction of three-dimensional brain models complicating the research algorithm (19-21,25,30). For the present study, we used a two-dimensional box-counting algorithm which includes fractal analysis of two-dimensional tomographic image sections (15,22). This method has its own advantages. We chose this method to evaluate the informativeness of a simpler and more accessible fractal analysis algorithm that does not require the construction of three-dimensional brain models. In some cases, three-dimensional brain model construction is difficult or impossible (due to too thick tomographic sections or poor MR image quality). In addition, sometimes it is necessary to assess only a certain brain area (for example, one particular tomographic

section) and compare the obtained FD value with values measured in adjacent areas to reveal and assess the changes in the region of interest. In such cases, it is advisable to use a two-dimensional box-counting algorithm. Kalmanti and Maris (22) in their study said that “interpretation of two-dimensional pictures is common in everyday medical practice and measurement of two-dimensional FD can easily be used since it does not need complicated volumetric methods and can indicate a threshold between normal as well as pathological changes”. In our opinion, a two-dimensional box-counting algorithm is more accessible and convenient for routine medical practice than a three-dimensional one.

As the object of the present study, we chose cerebral silhouettes. The quantitative assessment of the silhouette images makes it possible to simplify morphometric studies of cerebral hemispheres since it does not require the segmentation of brain tissue into constituent components (white and gray matter) and does not require the construction of three-dimensional brain models. The segmentation of brain tissue into white and gray matter usually requires special software and high-quality MR images. In some cases, the quality of routine MRI used in clinical practice is not good enough for this type of segmentation. Silhouettes obtained in our study weren't divided into components and included both cerebral tissue components, gray and white matter. The segmentation used in our study is simpler and more accessible for medical practitioners and it does not require high-quality MR images. Thus, the morphometric method used by us is more convenient for use in cases where segmentation of white and gray matter is not possible, or the thickness of the tomographic sections is not small enough to construct and quantify three-dimensional brain models.

Silhouettes obtained as a result of the segmentation of MR brain images make it possible to assess the spatial location of the brain tissues, its spatial configuration, and the space-filling degree. Age-related atrophic changes lead to a decrease in the volumes of white and gray matter, which is manifested in the shape changes of the cerebral hemispheres; the widening and deepening of the sulci, the reduction and simplification of the gyri may be found in the aged brain (3-5,21). These changes lead to a decrease in the intracranial volume filled with brain structures. At the same time, the percentage of intracranial space corresponding to the space inside the widened and deepened sulci (cerebrospinal fluid-filled space) increases (21). Thus, aging changes are associated with a decrease in the space-filling capacity of the cerebrum. In addition, atrophic changes lead to a simplification of the shape of the brain as a whole, which is reflected in the decrease in the complexity of the brain spatial configuration. FD is a parameter of fractal geometry that quantitatively characterizes the degree of space-filling and the complexity of the spatial configuration of the studied structures. Therefore, the FD of silhouette brain images is the appropriate morphometric parameter, which provides a specific and objective assessment of age-related changes in the shape of cerebral hemispheres.

Fractal analysis of the cerebral silhouettes of young and old persons gave us significantly different FD values. Thus, the FD of silhouette images proved to be a

sufficiently sensitive indicator to quantitatively distinguish two images, without atrophy and with age-related atrophic changes and to quantify the degree of atrophic changes. Based on the age and the FD values of the studied sample, we have calculated confidence intervals of the FD values of cerebral hemispheres silhouette images, which can be used as norm criteria in clinical neuroimaging.

The study of Podgórski et al (12) focused on the comparative analysis of brain aging in males and females. The authors found that FD, volumes of total gray matter, white matter, cerebrospinal fluid, cortical thickness, sulcal depth, gyrification index, and FD were changed during aging in both males and females. The study results showed that cortical FDs were changed during aging only in a small number of locations in males (2.0%), while that number was significantly higher in females (2.7%). Authors stated that male and female brains start aging at a similar age of 45, but compared to males, in females, the cortex is affected earlier and in a more complex pattern. Sex differences in brain age-related FD changes were also evaluated in the study of Farahibozorg et al. (30). This study focused on cerebral white matter. Researchers revealed that the interaction of age- and sex-dependent differences were significant mainly in the hemispheric analysis, the age-related changes were sharper in males. The authors noticed that after adjusting for the volume effect, age-related results remained approximately the same, but females had higher values, specifically in the left hemisphere and boundaries.

Our study also has revealed a decrease in FD values during life in males and females, but there are some differences between the present study and mentioned studies (12,30). The fractal analysis algorithms were quite different. In the study of Podgórski et al. (12) cortical FD maps were obtained, the study of Farahibozorg et al. (30) included fractal analysis of three-dimensional models of cerebral white matter, and the present study included analysis of two-dimensional cerebral silhouettes. Our study has shown no significant differences in the character of male and female brain aging. We revealed a continuous and gradual type of FD decrease during aging in both males and females. The character and strength of correlations between FD and age were similar in male and female groups. Some differences in correlation coefficients (between age and FD in male and female groups) can be explained by data heterogeneity and a relatively small sample size. Taking into account the absence of a significant difference between linear regression equations characterizing FD dynamics throughout life in males and females, we can conclude that there are no significant sex differences in the character of age-related brain changes estimated by fractal analysis of cerebral silhouettes.

CONCLUSION

Fractal analysis of silhouette MR images of the cerebral hemispheres has revealed and quantified age-associated changes in the brain spatial complexity and space-filling degree that characterize atrophic changes in normal aging. The obtained data can be used as normal criteria for assessing the degree of age-related cerebral atrophy and for differentiating between normal aging and neurodegenerative diseases.

Ethics Committee Approval: The study was approved by the Ethics Committee of Kharkiv National Medical University (07.11.2018, 10).

Conflict of Interest: None declared by the authors.

Financial Disclosure: None declared by the authors.

Acknowledgments: None declared by the authors.

Author Contributions: Idea/Concept: NM, OS; Design: NM, OS; Data Collection/Processing: NM; Analysis/Interpretation: NM, OS; Literature Review: NM; Drafting/Writing: NM; Critical Review: OS.

REFERENCES

- Mandelbrot BB. The fractal geometry of nature. San Francisco: W.H. Freeman and Company; 1982.
- Di Ieva A, Esteban FJ, Grizzi F, Klonowski W, Martín-Landrove M. Fractals in the neurosciences, Part II: clinical applications and future perspectives. *Neuroscientist*. 2015;21(1):30-43.
- Fjell AM, Walhovd KB. Structural brain changes in aging: courses, causes and cognitive consequences. *Rev Neurosci*. 2010;21(3):187-221.
- MacDonald ME, Pike GB. MRI of healthy brain aging: A review. *NMR Biomed*. 2021;34(9):e4564.
- Ota Y, Shah G. Imaging of normal brain aging. *Neuroimaging Clin N Am*. 2022;32(3):683-98.
- Pini L, Pievani M, Bocchetta M, Altomare D, Bosco P, Cavado E, et al. Brain atrophy in Alzheimer's disease and aging. *Ageing Res Rev*. 2016;30:25-48.
- Ertekin A. Brain white matter hyperintensity changes associated with vascular cognitive impairment and dementia, Alzheimer's dementia and normal aging. *Duzce Med J*. 2021;23(3):305-12.
- Ge Y, Grossman RI, Babb JS, Rabin ML, Mannon LJ, Kolson DL. Age-related total gray matter and white matter changes in normal adult brain. Part I: volumetric MR imaging analysis. *AJNR Am J Neuroradiol*. 2002;23(8):1327-33.
- Walhovd KB, Fjell AM, Reinvang I, Lundervold A, Dale AM, Eilertsen DE, et al. Effects of age on volumes of cortex, white matter and subcortical structures. *Neurobiol Aging*. 2005;26(9):1261-70; discussion 1275-8.
- Riello R, Sabattoli F, Beltramello A, Bonetti M, Bono G, Falini A, et al. Brain volumes in healthy adults aged 40 years and over: a voxel-based morphometry study. *Aging Clin Exp Res*. 2005;17(4):329-36.
- Zheng F, Liu Y, Yuan Z, Gao X, He Y, Liu X, et al. Age-related changes in cortical and subcortical structures of healthy adult brains: A surface-based morphometry study. *J Magn Reson Imaging*. 2019;49(1):152-63.
- Podgórski P, Bładowska J, Sasiadek M, Zimny A. Novel volumetric and surface-based magnetic resonance indices of the aging brain - does male and female brain age in the same way? *Front Neurol*. 2021;12:645729.
- Li Z, Zhang J, Wang F, Yang Y, Hu J, Li Q, et al. Surface-based morphometry study of the brain in

- benign childhood epilepsy with centrotemporal spikes. *Ann Transl Med.* 2020;8(18):1150.
14. Hofman MA. The fractal geometry of convoluted brains. *J Hirnforsch.* 1991;32(1):103-11.
 15. King RD, George AT, Jeon T, Hynan LS, Youn TS, Kennedy DN, et al. Characterization of atrophic changes in the cerebral cortex using fractal dimensional analysis. *Brain Imaging Behav.* 2009;3(2):154-66.
 16. Kiselev VG, Hahn KR, Auer DP. Is the brain cortex a fractal? *Neuroimage.* 2003;20(3):1765-74.
 17. Esteban FJ, Sepulcre J, de Miras JR, Navas J, de Mendizábal NV, Goñi J, et al. Fractal dimension analysis of grey matter in multiple sclerosis. *J Neurol Sci.* 2009;282(1-2):67-71.
 18. Roura E, Maclair G, Andorrà M, Juanals F, Pulido-Valdeolivas I, Saiz A, et al. Cortical fractal dimension predicts disability worsening in Multiple Sclerosis patients. *Neuroimage Clin.* 2021;30:102653.
 19. King RD, Brown B, Hwang M, Jeon T, George AT, Alzheimer's Disease Neuroimaging Initiative. Fractal dimension analysis of the cortical ribbon in mild Alzheimer's disease. *Neuroimage.* 2010;53(2):471-9.
 20. Goñi J, Sporns O, Cheng H, Aznárez-Sanado M, Wang Y, Josa S, et al. Robust estimation of fractal measures for characterizing the structural complexity of the human brain: optimization and reproducibility. *Neuroimage.* 2013;83:646-57.
 21. Madan CR, Kensinger EA. Cortical complexity as a measure of age-related brain atrophy. *Neuroimage.* 2016;134:617-29.
 22. Kalmanti E, Maris TG. Fractal dimension as an index of brain cortical changes throughout life. *In Vivo.* 2007;21(4):641-6.
 23. Ha TH, Yoon U, Lee KJ, Shin YW, Lee JM, Kim IY, et al. Fractal dimension of cerebral cortical surface in schizophrenia and obsessive-compulsive disorder. *Neurosci Lett.* 2005;384(1-2):172-6.
 24. Zhuo C, Li G, Chen C, Ji F, Lin X, Jiang D, et al. Left cerebral cortex complexity differences in sporadic healthy individuals with auditory verbal hallucinations: A pilot study. *Psychiatry Res.* 2020;285:112834.
 25. Im K, Lee JM, Yoon U, Shin YW, Hong SB, Kim IY, et al. Fractal dimension in human cortical surface: multiple regression analysis with cortical thickness, sulcal depth, and folding area. *Hum Brain Mapp.* 2006;27(12):994-1003.
 26. Lee JM, Yoon U, Kim JJ, Kim IY, Lee DS, Kwon JS, Kim SI. Analysis of the hemispheric asymmetry using fractal dimension of a skeletonized cerebral surface. *IEEE Trans Biomed Eng.* 2004;51(8):1494-8.
 27. Esteban FJ, Sepulcre J, de Mendizábal NV, Goñi J, Navas J, de Miras JR, et al. Fractal dimension and white matter changes in multiple sclerosis. *Neuroimage.* 2007;36(3):543-9.
 28. Rajagopalan V, Das A, Zhang L, Hillary F, Wylie GR, Yue GH. Fractal dimension brain morphometry: a novel approach to quantify white matter in traumatic brain injury. *Brain Imaging Behav.* 2019;13(4):914-24.
 29. Zhang L, Dean D, Liu JZ, Sahgal V, Wang X, Yue GH. Quantifying degeneration of white matter in normal aging using fractal dimension. *Neurobiol Aging.* 2007;28(10):1543-55.
 30. Farahibozorg S, Hashemi-Golpayegani SM, Ashburner J. Age- and sex-related variations in the brain white matter fractal dimension throughout adulthood: an MRI study. *Clin Neuroradiol.* 2015;25(1):19-32.
 31. Zhang L, Liu JZ, Dean D, Sahgal V, Yue GH. A three-dimensional fractal analysis method for quantifying white matter structure in human brain. *J Neurosci Methods.* 2006;150(2):242-53.
 32. Schneider CA, Rasband WS, Eliceiri KW. NIH Image to ImageJ: 25 years of image analysis. *Nat Methods.* 2012;9(7):671-5.
 33. Underwood EE. *Quantitative stereology.* Reading, Massachusetts: Addison-Wesley; 1970.